Available online at www.sciencedirect.com
SCIENCE DIRECT®
Journal of Chromatography A, 1087 (2005) 158–168
JOURNAL OF CHROMATOGRAPHY A
www.elsevier.com/locate/chroma

Inverse gas chromatographic investigation of the effect of hydrogen in carbon monoxide adsorption over silica supported Rh and Pt–Rh alloy catalysts, under hydrogen-rich conditions☆

Dimitrios Gavril*, Vassilios Loukopoulos, Aglaia Georgaka, Aristea Gabriel, George Karaiskakis

Physical Chemistry Laboratory, Department of Chemistry, University of Patras, 26504 Patras, Greece

Available online 31 May 2005

Abstract

Selective CO oxidation (SCO) has attracted scientific and technological interest due to its application to the operation of proton electrolyte membrane fuel cells (PEM-FCs). CO adsorption, being an elementary step of SCO, is studied over silica supported monometallic Rh and $Rh_{0.50} + Pt_{0.50}$ alloy catalysts, under various hydrogen atmospheres, namely: 25% H_2 + 75% He, 50% H_2 + 50% He and 75% H_2 + 25% He carrier gas mixture compositions. The investigation of CO adsorption is done by utilizing reversed-flow gas chromatography (RF-GC). As a result rate constants for the adsorption (k_1), desorption (k_{-1}) and irreversible CO binding (k_2) over the studied catalysts as well as the respective activation energies are determined. The variation of the rate constants and the activation energies against the nature of the used catalyst (monometalic or alloy) and the amount of hydrogen in the carrier gas gives useful information for the selectivity as well as the activity of CO oxidation over group VIII noble metals. At low temperatures and under H_2-rich conditions compatible with the operation of PEM fuel cells the activity of the monometallic and the alloy catalysts is expected to be similar, however the selectivity of $Rh_{0.50} + Pt_{0.50}$ alloy catalyst is expected to be higher, making Pt–Rh alloy catalyst as a better candidate for CO preferential oxidation (PROX). The low energy barrier values found in the present work, most likely are referred to high surface amounts of CO. The desorption barriers determined are in any case much lower than the respective activation energies found for CO desorption in the absence of hydrogen indicating a H_2-induced desorption, which can explain the observed in the literature rate enhancement of SCO oxidation.

Keywords: Inverse gas chromatography; Physicochemical measurements; PEM fuel-cells; Platinum–Rhodium alloy catalysts; Selective CO oxidation (SCO); Preferential oxidation (PROX); Activity; Selectivity

1. Introduction

Fuel cells are developed as a viable alternative for clean energy generation. Fuel cell technology applications vary from portable/micro power and transportation through to stationary power for buildings and distributed generation. Various fuel cells applications operating at different temperatures have been developed [1]. A series of advantages such as: low operating temperature (343–373 K), low weight, compactness, long stack life, suitability to discontinuous operation as well as potential for low cost make proton exchange membrane (PEM) fuel cells leading candidates for mobile power and/or for small power units' applications.

The rational operation of the fuel cell units is closely related to the development of very active poison-resistant and selective catalysts, which result in small catalytic volumes, durability under steady-state and transient conditions, low cost and versatility to variations in fuel/feed composition.

Pure hydrogen is the ideal fuel for the PEM fuel cell. However, there is no available technology for safely storing enough hydrogen to give a PEM fuel cell powered vehicle acceptable range. PEM fuel cells utilize the hydrogen produced by external reforming using steam, air or a combination of both. Steam reforming, catalytic partial oxidation and au-

☆ Presented at the 25 ISC, Paris, October 4–8, 2004.

* Corresponding author. Fax: +30 2610997144.
E-mail address: d.gavril@upatras.gr (D. Gavril).

0021-9673/$ – see front matter © 2005 Elsevier B.V. All rights reserved.
doi:10.1016/j.chroma.2005.04.065

tothermal reforming are used for reforming fuels and produce syngas (a mixture of carbon monoxide and hydrogen) as well as water–gas shift reaction consumes carbon monoxide and water vapours to produce more hydrogen and carbon dioxide. The resulting hydrogen-rich stream gas mixture containing 40–75% H_2, 15–25% CO_2, 15–30% H_2O and 0–25% N_2, it is however contaminated with 0.5–1% of CO. Trace amounts of carbon monoxide in the hydrogen-rich stream deteriorate the efficiency of the PEM fuel cell by poisoning the platinum (or Pt–Ru) anode, accelerated at CO levels higher than 50 ppm. Selective carbon monoxide oxidation (SCO) also referred as preferential oxidation (PROX), is considered to be the most promising and lowest cost approach without excessive hydrogen consumption [2].

An efficient SCO catalyst must be highly active in CO oxidation at temperatures compatible with the operation of PEM fuel cells (343–373 K) and very selective towards CO_2 formation. For a number of reasons these catalyst requirements, high activity in CO oxidation at the temperature range: 343–373 K and almost no hydrogen oxidation are hard to meet because hydrogen oxidation is faster than carbon monoxide oxidation on most of the noble metal catalysts, and in the relevant temperature range CO oxidation is very slow on Pt and Pd (more usual active catalysts used for CO oxidation) due to CO inhibition [3].

While CO oxidation over group VIII noble metals is the most studied catalytic reaction, selective oxidation of CO in hydrogen-rich conditions is not nearly as well studied. It has been observed that hydrogen oxidation (undesirable) is strongly inhibited by the presence of CO (CO inhibition) in the reactant stream due to the higher sticking coefficient of CO on noble metal surfaces compared to those of H_2 or O_2 [2–4]. Similarly to that encountered during CO oxidation in the absence of H_2 the onset of the reaction both in the presence and absence of H_2 in the feed is controlled by CO desorption [2]. Moreover, it has been observed that hydrogen and water vapors enhance CO oxidation over Pt catalysts and consequently decrease the respective activation energy [3]. However, the amount of hydrogen in the H_2-rich stream varies from 40 to 75%. CO adsorption is a fundamental step for SCO and the kinetic investigation of the effect of different hydrogen amounts in CO adsorption rate over supported noble metal catalysts is a subject of great interest, and the influence of different hydrogen compositions has never been studied, in our knowledge.

In the present study, CO adsorption is investigated over a monometalic silica supported rhodium and a bimetallic $Rh_{0.50} + Pt_{0.50}$ catalysts, under various hydrogen atmospheres, namely: 25–75% H_2. Rh/SiO_2 catalyst selected since supported Rh has been found to combine high CO selectivity and satisfactory activity compared to a supported Pt catalyst, in conditions compatible with the operation of PEM fuel cells [2]. On the other hand bimetallic $Rh_{0.50} + Pt_{0.50}/SiO_2$ catalyst selection based on the facts that Pt–Rh alloy catalysts exhibit high activity for CO oxidation at lower temperatures than the monometallic ones (Pt–Rh synergism) [5,6], as well as various Pt based alloys have been proposed to alleviate CO inhibition problem due to their CO tolerance. In that case alloying may change the chemical properties of the Pt atoms in the surface (ligand effect), resulting in a weaker CO binding and consequently smaller CO coverage and weaker CO poisoning effect [4].

The comparison of the physicochemical quantities of the present work determined in the absence of oxygen with those of SCO in the presence of oxygen is utilized from the observed CO inhibitive (or poisoning/covering) effect. Thus, at low temperatures compatible with the operation of proton electrolyte membrane fuel cells, hydrogen oxidation (undesirable) and CO oxidation (desirable) are inhibited in a different degree due to the fact that sufficient amounts of oxygen cannot be dissociatively adsorbed on the surface. Thus, considering the simpler form of SCO, e.g. a reactant stream containing traces of CO and oxygen in excess of hydrogen over noble metal catalysts, the onset of selective CO oxidation is controlled again by CO desorption, as in the case of CO oxidation. Furthermore, the comparison of our data is further utilized from the fact that oxygen adsorption/dissociation is much more influenced by CO adsorption than vice-versa due to CO poisoning effect.

In this work the use of reversed-flow gas chromatography (RF-GC) technique is extended in adsorption studies under conditions compatible with the operation of PEM fuel cells. RF-GC is not limited to chromatographic separation, since it is accompanied by suitable mathematical analysis of the chromatographic data which makes possible the simultaneous determination of various physicochemical parameters related to the kinetics of the elementary steps (adsorption, desorption, surface reaction) and the nature of the active sites [5–10].

RF-GC methodologies have been used during the last decade for the investigation of the adsorption of CO, O_2 and CO_2 as well as the oxidation of CO over well studied silica supported Pt, Rh and Pt–Rh bimetallic catalysts [5–10]. The experimental findings by means of RF-GC are in agreement with those obtained with different techniques and methodologies, for the same catalysts ascertaining the potential of RF-GC for reliable and accurate catalytic characterizations.

Thus various processes and the consequent physicochemical parameters have been successfully studied: (i) time depended, X_t, and overall, X, conversions, either under steady or non steady state conditions [5,6], (ii) adsorption, k_1, desorption, k_{-1}, and surface reaction, k_2, rate constants and the respective activation energies, E_a [6], (iii) local adsorption energies, ε, local adsorption isotherms, $\theta(p, T, \varepsilon)$, local monolayer capacities, c^*_{max}, and adsorption energy distribution functions, $f(\varepsilon)$, for the adsorption of gases on heterogeneous surfaces [7–9], (iv) the energy of the lateral molecular interactions on heterogeneous surfaces in a time resolved procedure as well as surface diffusion coefficients for physically adsorbed or chemisorbed species on heterogeneous surfaces in a time resolved procedure [9], (v) the nature of the various groups of active sites of solid catalysts [9] and the competition between mass transfer and kinetics on solid catalysts [10].

2. Experimental

2.1. General

Conventional GC involves the flow of a gaseous mobile phase in a defined direction over a stationary phase or packing that results in the selective retention of solute components. In RF-GC the system is modified (c.f. Fig. 1), having placed perpendicularly in the center of the chromatographic column (sampling column) another column (diffusion column). The carrier gas flows continuously through the sampling column, while it is stagnant into the diffusion column. In contrast with conventional GC, where the mobile phase is the center of interest, in RF-GC the solid or liquid substance placed into the diffusion column is under investigation. Thus, RF-GC can be assumed as an inverse gas chromatographic method. The injection of the solute is done at the closed end of the diffusion column. Thus, the displacement of the injected solute into the diffusion column is only affected by its interaction with the stationary phase and its diffusion into the stagnant carrier gas.

Another peculiarity of RF-GC is the sampling procedure of the physicochemical phenomenon, which happens into the diffusion column. The sampling procedure is carried out by using a four or six-port valve. Carrier gas flow reversals, for a short time interval, are done by means of the above-mentioned valve, and then the flow is restored in its original direction. The above-described flow reversals result in a short enrichment of the solute quantity into the carrier gas and extra chromatographic peaks are created on the continuous concentration-time curve (chromatogram). The extra peaks are symmetrical and their height or area is proportional to the concentration of the solute in the junction of the diffusion and sampling columns, giving to RF-GC a higher sensitivity and accuracy. The estimation of the various parameters is done from plots of the heights or the areas of the extra chromatographic peaks against the time from solute's injection (which are so-called as Diffusion Bands) and from geometrical characteristics of the diffusion column (such as its length and its volume).

The materials and apparatus used for the study of carbon monoxide adsorption under various carrier gas hydrogen amounts, by RF-GC, have been presented in detail in previous publications [7]. A short description of them follows.

2.2. Materials

The catalysts studied, were rhodium and a $Pt_{0.50} + Rh_{0.50}$ alloy (3%, w/w) supported on silica gel 60 of Merck (Darmstadt, Germany), $d < 0.063$ mm, 70–230 mesh ASTM. The method of preparation and the surface characterization of the catalysts using TDS and XPS, has been presented previously [11].

Silica gel (80–100 mesh) from Supelco (Bellfonte, Pennsylvania) was used as chromatographic material for the separation of carbon monoxide and carbon dioxide.

Hydrogen, from Linde (Patras, Greece) (99.999% pure) was used for the reduction of the catalysts, while helium, from BOC Gases (Athens, Greece) (99.999% pure) was used as carrier gas.

Carbon monoxide from B.O.C. Gases (Athens, Greece) (99.997% pure), was used as adsorbate.

In order to examine the change of CO adsorption with hydrogen amount, three different composition hydrogen/helium mixtures were prepared by B.O.C. Gases (Germany) and were used as carrier gases. Their compositions were: 25.05% H_2 + 74.95% He (v/v, 99.999% pure), 49.95% H_2 + 50.05% He (v/v, 99.999% pure) and 75.05% H_2 + 24.95% He (v/v, 99.999% pure).

The actual gas mixture concentrations were measured by a gas chromatograph Perkin-Elmer XL Autosystem with a TC detector by using a 3 m column filled with Molecular Sieve 5A. The working temperature was 333 K, while the flow rate of the carrier gas Ar was 20 ml min^{-1}.

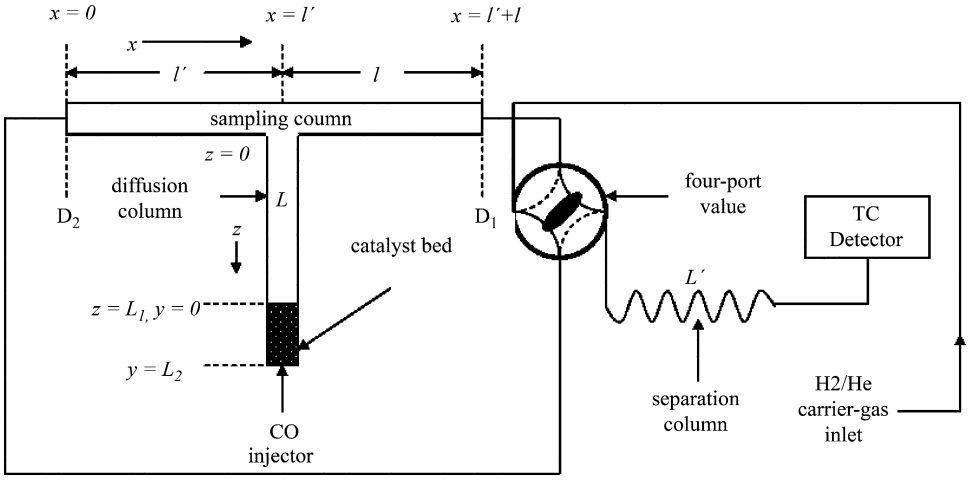

Fig. 1. Experimental setup used for the investigation of the effect of hydrogen in carbon monoxide adsorption over silica supported Rh and Pt–Rh alloy catalysts, under hydrogen-rich conditions, from reversed-flow gas chromatography.

2.3. Apparatus

The lengths l', l and L of the stainless-steel "*sampling cell*" were incorporated into a commercial gas chromatograph, Shimadzu GC-8A, equipped with a thermal conductivity detector as shown in Fig. 1. The lengths l' and l of the sampling column were 36.5 cm each (4 mm i.d.), while the length L of the diffusion column was 70 cm (4 mm i.d.). The catalytic bed (0.09 g) was put in a 1 cm length at the top of diffusion column L. The separation column, L' (4 mm i.d.), was filled with 7.6 g of silica gel (80–100 mesh).

2.4. Procedure

Before any use, the catalysts were reduced at 628 K for 10 h in flowing hydrogen, at a flow rate of 1.137 $cm^3\ s^{-1}$. After, the whole system was conditioned by heating "in situ" the catalyst bed at 748 K for 20 h, under continuous carrier gas flow. Some preliminary injections of the adsorbate (CO) were made to stabilize the adsorptive behaviour. Then, 1.0 cm^3 of the solute (carbon monoxide), under atmospheric pressure was rapidly introduced, with a gas-tight syringe, at the top of the diffusion column L, with the carrier gas flowing in direction from D_1 to D_2 (Fig. 1). After a time of 5 min, a continuous concentration–time curve, owing to CO was established and recorded. As it was pointed out before, during this period flow reversals of carrier gas direction, for 5 s, were made and then the gas was again turned to its original direction, simply by switching the four-port valve from one position to the other and vice-versa. This time period was shorter than the gas hold-up time in column sections l', l and L'. When the gas flow was restored to its original direction CO sample peaks like those of Fig. 2 were recorded. Repeating the reversal procedure many times at each experiment, a series of sample peaks were recorded; each of them was corresponded to a different time from adsorbate's injection. Result of the reversals is the instantaneous enrichment of the carrier gas at the junction of diffusion and sampling columns, with the injected solute. The carrier gas performs only the sampling procedure to measure the gas phase concentration of an analyte at a certain position as function of time, while it is stagnant into the diffusion column L.

Plot of the height of the sample peaks against the corresponding time from adsorbate's injection give the so-called "*diffusion band*", shown in Fig. 3 of ref. [7], and from its mathematical analysis the various physicochemical parameters are estimated.

A Shimadzu C-R6A Chromatopac was used as recorder. The variation in the temperature along the catalytic bed was measured by a digital thermometer Fluke 2190A and was smaller than 1 K. The volumetric carrier gas flow rate, at ambient temperature was 1.136 $cm^3\ s^{-1}$. The pressure drop along the whole system was 0.414 atm.

3. Theoretical

The sampling peaks are predicted theoretically by the "chromatographic sampling equation" describing the concentration–time curve that it is recorded after each flow reversal. The area, A, or the height, H, of the sample peaks resulting from the flow reversals, measured as function of time, t, are proportional to the concentration of the substance under study, at the junction, $x = l'$, of the sampling cell, at time, t, $c(l', t)$:

$$H^{1/M} = gc(l', t) \quad (1)$$

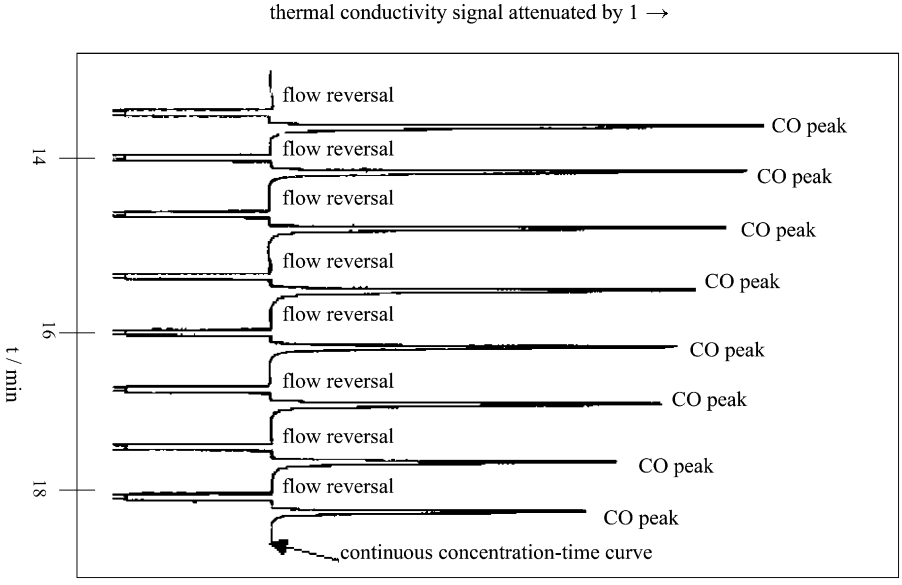

Fig. 2. Reversed-flow gas chromatogram showing "sampling peaks", for the sorption of CO at 100.0 °C, over Rh/SiO_2 catalyst, under a 75% H_2 + 25% He carrier gas atmosphere.

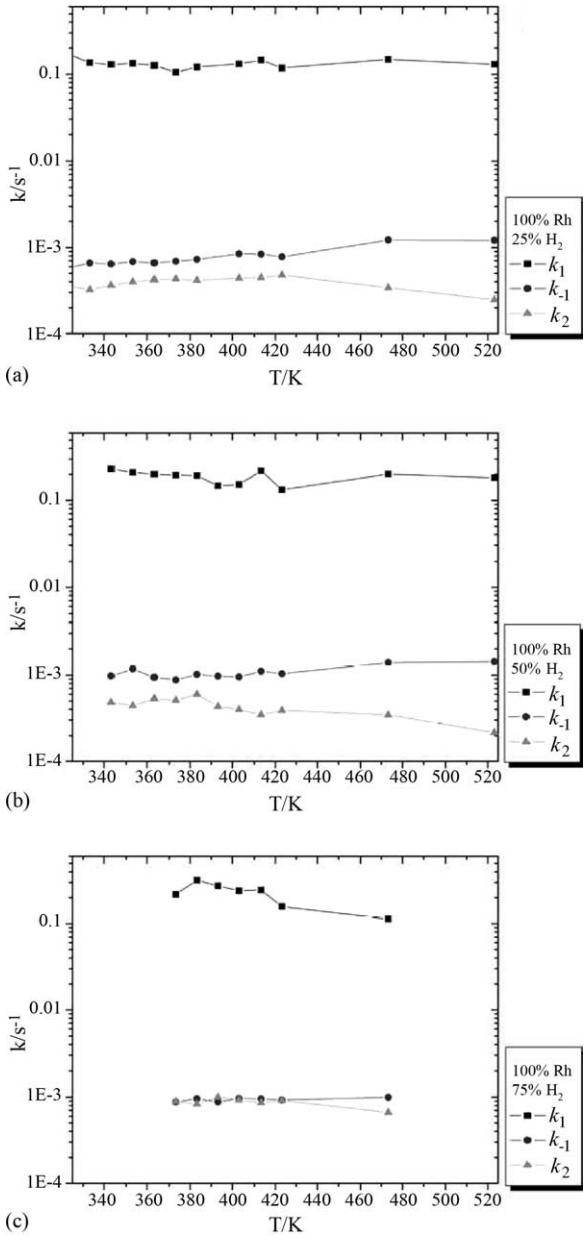

Fig. 3. Temperature variation of the mean values of the rate constants (s^{-1}), in a semi-logarithmic scale, for the adsorption, k_1, desorption, k_{-1}, and surface binding, k_2, of carbon monoxide over silica supported rhodium catalyst at (a) 25% H_2, (b) 50% H_2, and (c) 75% H_2.

where M is the response factor of the detector and g a proportionality constant (usually assumed equal to unity) pertaining to the detector calibration. Measuring experimentally pairs H, t, the diffusion band is constructed, which in the case of a solute adsorption is theoretically described by the sum of two exponential functions of time [5–10]:

$$H^{1/M} = N\left(1+\frac{Z}{Y}\right)\exp\left(-\frac{X+Y}{2}t\right) + N\left(1-\frac{Z}{Y}\right)\exp\left(-\frac{X-Y}{2}t\right) \quad (2)$$

N is a function of the amount of the injected adsorbate, of the carrier gas volumetric flow-rate, of the geometrical characteristics of the diffusion column and of the diffusivity of the adsorbate into the carrier gas. Its value, included in the pre-exponential factors of Eq. (2), is eliminated during the calculations.

The pre-exponential factors, $A_1 = N(1-(Z/Y))$, $A_2 = N(1+(Z/Y))$ and the exponential coefficients of time $B_1 = -(X-Y)/2$ and $B_2 = -(X+Y)/2$, are calculated by a non-linear regression analysis program [6].

The auxiliary parameters X, Y and Z are functions of the rate constants k_1, k_{-1} and k_2 as well as of the geometric characteristics of the diffusion column and the diffusivity of the adsorbate into the carrier gas. By adding the two exponential coefficients of time B_1 and B_2, the value of X is found, while subtracting B_1 and B_2, the value of Y is obtained. The value of Z is found from the ratio of the two pre-exponential factors A_1 and A_2 ($\rho = A_1/A_2$):

$$Z = \left(\frac{1-\rho}{1+\rho}\right)Y \quad (3)$$

Finally, the rate constants for adsorption, k_1, desorption, k_{-1} and irreversible surface binding, k_2 can be calculated from the found values of X, Y and Z, by means of the following relations [6]:

$$k_1 = \frac{(X+Z)(1+V_1)-2a_1}{2V_1} \quad (4)$$

$$k_{-1} = \frac{X-Z}{2} - k_2 \quad (5)$$

$$k_2 = \frac{(X^2-Y^2)(1+V_1)-2a_1(X-Z)}{2(X+Z)(1+V_1)-4a_1} \quad (6)$$

$$a_2 = \frac{2D}{L_2^2} \quad (7)$$

$$V_1 = 2\frac{V'_G\varepsilon}{V_G} + \frac{a_1}{a_2} \quad (8)$$

In the above equations, V_G and V'_G are the gaseous volumes of empty sections L_1 and L_2, respectively, a_1, a_2 functions of the diffusion coefficient, D, of carbon monoxide at the experimental temperature and pressure and ε is the external porosity of catalyst bed.

Eqs. (4)–(6) show that for the calculation of the rate constants k_1, k_{-1} and k_2, the following parameters are required: (i) The auxiliary parameters X, Y and Z determined by the pre-exponential factors and exponential coefficients of Eq. (2), which are easily calculated by non linear regression analysis of the diffusion band. (ii) The diffusion coefficient of CO, D. The determination of diffusion coefficients can be done either experimentally [12] or theoretically. (iii) The parameter V_1 defined by Eq. (8), is easily calculated by the geometric properties of the diffusion column and the value of the diffusion coefficient of CO, D. (iv) The external porosity of the

catalyst bed, ε, which can be measured by a method described elsewhere [13].

The rate constants k_1, k_{-1} and k_2 relate to non steady state conditions and they are well distinguished from diffusion rates.

4. Results and discussion

The working temperature for the kinetic experiments was limited between 323 and 523 K. In this temperature range the only recorded substance is carbon monoxide. The existence of other possible products of CO adsorption in excess of hydrogen such as H_2O, CO_2 and CH_4 into the carrier gas, due to either possible CO dissociative adsorption or methanation reaction, was examined as follows: (a) the carrier gas stream was passed through a molecular sieve 5A water vapour trap; (b) a silica gel 80–100 mesh column (60 cm length, 1/4″ o.d.) was put in before the TC detector. This column was used for the separation of CO and CO_2, and (c) finally, the carrier gas stream was also passed through a FID detector, for the detection of hydrocarbons (e.g. CH_4). The only detectable substance was carbon monoxide.

Furthermore, the experimental findings for the adsorption of CO on the studied catalysts in the absence of hydrogen show that it is a dissociative process, at temperatures higher than 553 K [6]. Moreover, the rate of methanation reaction is low in the studied temperature range (323–523 K) [3]. It has been shown that the methanation reaction in H_2/CO mixtures occurring at a very low rate on polycrystalline noble metals under atmospheric pressure can be enhanced if noble metals are supported on oxide materials. However, this support enhancement decreases in the order $TiO_2 > Al_2O_3 > SiO_2$ [3]. Consequently, the present kinetic investigation of CO adsorption in excess of hydrogen, over the studied silica supported Rh and Pt–Rh alloy catalysts, in the temperature range between 323 and 523 K, is not affected from both CO dissociative adsorption and CO methanation reaction.

The interaction of carbon monoxide with the studied catalysts can be outlined in the following mechanistic scheme in which the elementary reversible steps of adsorption, k_1, and desorption, k_{-1}, are followed by the possible irreversible surface binding, k_2.

$$CO_{(g)} \underset{k_{-1}}{\overset{k_1}{\rightleftarrows}} CO_{(ads)} \xrightarrow{k_2} CO_{(irr.,\ bind.)} \quad (9)$$

It is difficult to estimate the errors of the rate constants estimated from Eqs. (4)–(6), since they emerge from a series of a rather complex calculations and the application of the rule of error propagation in a long sequence of steps does not give reliable final errors. For this reason, the rate constants corresponding to the elementary processes of the interaction of CO with the studied catalysts have been determined by performing three consecutive experiments at each temperature. The found precision of the experimentally determined rates is satisfactory e.g. it was found that for CO adsorption over Rh/SiO_2 catalyst under 25% H_2, at 353 K: $k_1 = 0.133 \pm 0.006\ s^{-1}$ (4.5%), $k_{-1} = (6.845 \pm 0.045) \times 10^{-4}\ s^{-1}$ (6.6%) and $k_2 = (3.986 \pm 0.022) \times 10^{-4}\ s^{-1}$ (5.5%). The temperature variation of the mean values of the experimentally determined, by means of RF-GC, adsorption, k_1, desorption, k_{-1}, and irreversible surface binding, k_2, rate constants of carbon monoxide at three different hydrogen compositions on the two studied Rh/SiO_2 and $Pt_{0.50} + Rh_{0.50}/SiO_2$ catalysts is presented in Figs. 3 and 4, respectively.

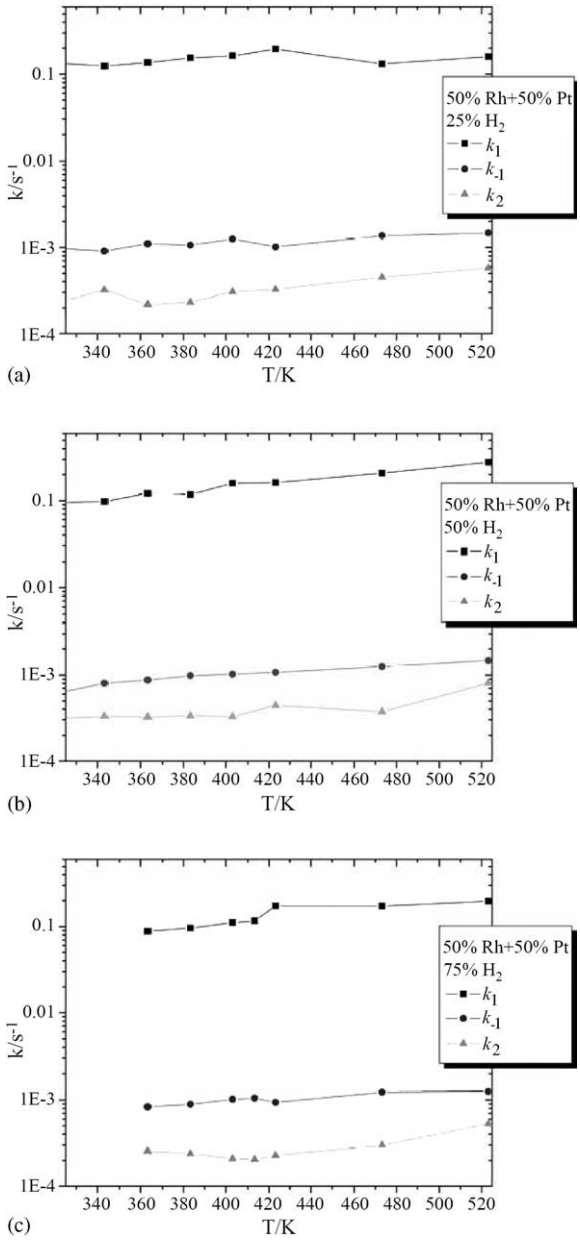

Fig. 4. Temperature variation of the mean values of the rate constants (s^{-1}), in a semi-logarithmic scale, for the adsorption, k_1, desorption, k_{-1}, and surface binding, k_2, of carbon monoxide over silica supported Pt–Rh alloy catalyst at (a) 25% H_2, (b) 50% H_2, and (c) 75% H_2.

It is generally suggested in the literature [2,3] that in excess of hydrogen over group VIII noble metals the strength of CO adsorption (k_2 values) determines the selectivity of CO oxidation, due to the well-known CO inhibition, while SCO activity is determined from CO desorption (k_{-1} values), which results in free active sites for the adsorption of other less weakly adsorbed species such as H_2 and O_2. Based on the fundamental CO blocking action, it is justifiable to utilize the measured by means of RF-GC rates related to the elementary steps of CO adsorption, desorption and irreversible binding over noble metal surfaces (Rh and Pt/Rh alloy) under various carrier gas hydrogen amounts (0–75%), in the absence of oxygen, in order to evaluate the activity and the selectivity of the studied catalysts for the simple case of SCO, i.e. a gaseous stream containing traces of CO and O_2 in excess of hydrogen.

The adsorption rate constant values, k_1, are usually two orders of magnitude higher than those of desorption, k_{-1}. The values of the experimentally determined adsorption rate constants are of the same order of magnitude compared with those determined by the frequency response method for the adsorption of CO on silica supported Pt catalysts [14], ascertaining the potential of RF-GC for accurate rate constants measurements. The deviation between adsorption and desorption values can be explained by means of the well-known high sticking coefficient of CO molecules over noble metals [2,3,9].

In all the cases the rate constants corresponding to the irreversible binding of CO, k_2, over the studied Pt-Rh catalysts, are lower than those of adsorption and desorption, with the exception of Rh/SiO_2 catalyst under 75% H_2. In that catalyst (Rh/SiO_2) the deviation between k_{-1} and k_2 values decreases with increasing hydrogen amounts, and particularly at the higher composition (75% H_2) both k_{-1} and k_2 values become almost equal. The deviation between k_{-1} and k_2 values can be attributed to the fact that the experimentally determined k_1 and k_{-1} values generally represent the transport rates of CO from the gas phase to the surface and from the surface to the gas phase, respectively. On the other hand the found k_2 values, corresponding to the surface binding of CO on the catalysts active sites, are referred to a state of a limited degree of freedom, in comparison with the rates of adsorption and desorption. Consequently, lower k_2 values are expected. Furthermore, lower k_2 values indicate a stronger interaction of CO molecules with catalyst active sites. Thus, for the monometallic catalyst, in which the deviation between k_{-1} and k_2 values decreases with increasing hydrogen amounts due to the drastic increase of k_2 values, the binding of CO molecules is expected to be weaker, particularly at higher hydrogen compositions.

It becomes obvious that at higher hydrogen compositions both the processes of CO adsorption and surface binding over the monometallic catalyst become relatively faster (from k_1 values) resulting in weaker interaction (from k_2 values) between CO and the studied catalyst active sites. This can also ascertained from the comparative presentation of the rates at a fixed temperature 373 K which is a relatively low temperature compatible with the operation of PEM fuel cells, and in which high selectivity and activity for SCO are expected by utilising supported Rh catalysts [2]. The variation of the adsorption, desorption and surface binding rate constants against the carrier-gas hydrogen percentage over the monometallic Rh as well as the bimetallic Pt-Rh catalysts, at 373 K is presented in Fig. 5.

The values of the adsorption rate, k_1, in the case of the monometallic Rh/SiO_2 catalyst increase, while the respective values of the bimetallic $Pt_{0.50} + Rh_{0.50}/SiO_2$ catalyst decrease with increasing carrier gas hydrogen amount. In any case, at hydrogen compositions compatible with the operation of low temperature PEM fuel cells (40–75% H_2) the rate of adsorption over monometallic catalyst is higher than that over the bimetallic catalyst ($k_1^{Rh} > k_1^{Pt\text{-}Rh}$) and moreover their deviation increases at higher H_2 compositions.

Surface binding rate values, k_2, provide a measure of the strength of the bond formed between adsorbed CO and catalyst active sites. Under any studied hydrogen composition, k_2 values corresponding to bimetallic Pt-Rh catalyst are lower than those of the monometallic catalyst ($k_2^{Pt\text{-}Rh} < k_1^{Rh}$) ascertaining that CO adsorption on Pt-Rh catalyst active sites is stronger than on Rh, which is consistent with the well-known preference of CO to adsorb on Pt sites [2–4,9,11]. Furthermore, similarly to adsorption rates, k_2 values in the case of the monometallic Rh/SiO_2 catalyst increase, while the respective values of the bimetallic catalyst decrease with increasing carrier gas hydrogen amount.

The selectivity of SCO towards CO_2 production is strongly enhanced by the stronger binding of CO on catalyst active sites, based on the well-known blocking action of CO to cover almost entirely the surface excluding hydrogen and oxygen from the active sites [2,3]. Although at lower hydrogen contents the CO selectivity of both catalysts determined from k_1 and k_2 values is similar, at rising H_2 carrier-gas contents such as in the range 40–75% H_2 which is compatible with the operation of PEM fuel cells, the variation of the rates of adsorption and surface binding indicates that the selectivity of the monometalic Rh catalyst is expected to decrease (increasing k_1 and k_2 values). In contrast, the CO selectivity of the Pt–Rh alloy is expected to increase at rising H_2 contents. Furthermore, the bimetallic $Pt_{0.50} + Rh_{0.50}/SiO_2$ catalyst is expected to be more selective at higher hydrogen compositions (lower k_2 values).

On the other hand, the activity of SCO is determined from carbon monoxide desorption resulting in more free active sites for the adsorption of weakly adsorbed species such as oxygen and hydrogen. At lower H_2 compositions, the rate of desorption from the bimetallic catalyst is higher than that of the monometallic catalyst ($k_{-1}^{Pt\text{-}Rh} > k_{-1}^{Rh}$), indicating that Pt–Rh alloy may be more active for SCO. At the range of the compatible with the operation of PEM fuel cells higher H_2 compositions (40–75% H_2), the values of the desorption rates become similar indicating a similar activity of both catalysts. Moreover, the activity of the bimetallic catalyst is expected to

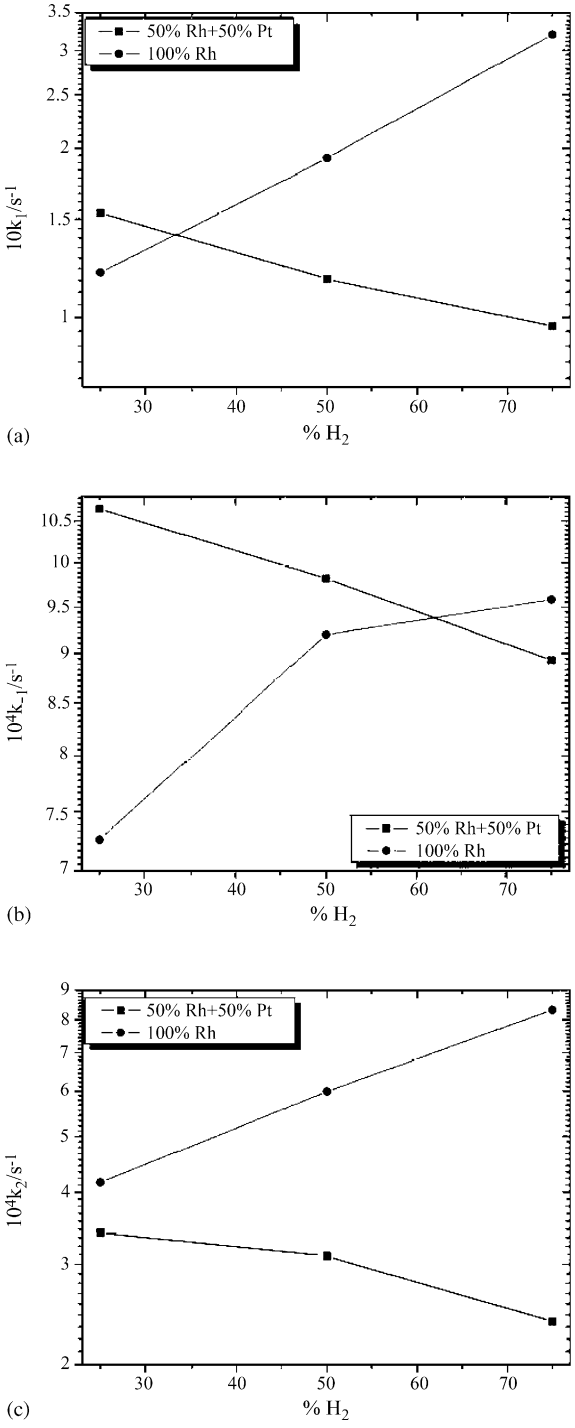

Fig. 5. Comparative presentation of the variation of the (a) adsorption, k_1, (b) desorption, k_{-1}, and (c) surface binding, k_2, rate constants, in a semi-logarithmic scale, of carbon monoxide over the two studied silica supported monometallic Rh and bimetallic Pt-Rh catalyst against the percentage of carrier-gas hydrogen (25–75% H_2).

decrease while that of the monometallic to increase at higher H_2 amounts.

The higher activity for CO oxidation of Pt–Rh alloys compared to monometallic Pt and Rh catalysts has been reported. The synergistic effect of Pt-Rh catalysts to exhibit higher catalytic activity for CO oxidation at lower temperatures is explained on the basis of the more random topography of the bimetallic catalyst compared to that of the pure Pt and Rh, to ensure the adsorption of CO molecules and O atom in the vicinity of each other [9].

The suggested CO tolerance of various Pt-based alloys is not directly ascertained on the studied Pt-Rh bimetallic catalyst due to the fact that comparable data for the adsorption of CO over a Pt/SiO_2 catalyst are not available. The influence of alloying in increasing the CO tolerance of Pt catalysts is attributed to a possible change of the chemical properties of the Pt atoms in the surface. In that case CO is bound more weakly and hence the CO poisoning effect weaker [4]. However, it is obvious from the higher k_2 values that CO is bound less strongly over Rh sites in comparison to Pt containing Pt–Rh alloy. Consequently, it can not be excluded that alloying Pt with Rh most likely results in a catalyst in which CO is bound weaker than on Pt actives sites and stronger than on Rh sites in agreement with the suggested CO tolerance of Pt-based alloys.

CO desorption is considered as the rate limiting step for CO oxidation both in the presence as well in the absence of hydrogen [2,3], consequently, the comparative variation of the desorption rates, k_{-1}, can give information for the activity of the studied catalysts. Desorption rates exhibit a similar behaviour at rising hydrogen compositions to those of adsorption and surface binding rates: they increase in the case of Rh/SiO_2 and decrease in the case of $Pt_{0.50} + Rh_{0.50}/SiO_2$ catalyst. Thus, adsorbed CO can easier desorb at higher H_2 contents, resulting in improvement of the activity and subsequent loss of selectivity of the monometallic Rh/SiO_2 catalyst for SCO. However, bearing also in mind that under the same rising H_2 conditions CO blocking effect increases, Rh/SiO_2 is expected to combine high selectivity as well as activity for SCO at low temperatures, as it has been observed [2].

In contrast, adsorbed CO desorption decreases from the bimetallic catalyst active sites, particularly at higher H_2 compositions resulting in the improvement of CO selectivity but also rising concerns about the activity of CO oxidation on Pt–Rh. However, in a big range of carrier-gas hydrogen compositions (25–60% H_2) the values of desorption rates of the bimetallic catalyst are sufficiently higher than the respective rates corresponding to the monometallic catalyst ($k_{-1}^{\text{Pt-Rh}} > k_{-1}^{\text{Rh}}$), while at higher compositions the desorption rates become similar. Thus, the loss of activity is not expected to be significant compared to that of the pure Rh catalyst.

For all the studied catalysts the values of the desorption rate constants, k_{-1}, increase with increasing temperature indicating that the relevant process is activated and permitting the calculation of the corresponding activation energies via the Arrhenius equation. Bearing in mind that carbon monoxide desorption plays a crucial role in CO oxidation both in the presence as well in the absence of hydrogen [2,3], the comparison of the respective activation energies against the nature of the studied catalysts (monometallic or bimetallic) will further enlighten the activity of these catalysts.

On the other hand, the rate constants, corresponding to CO adsorption, k_1, over the monometallic rhodium catalyst decrease under any hydrogen atmosphere. The same behaviour is also exhibited by the irreversible binding rates, k_2, over the same pure rhodium catalyst with the exception of the lower 25% hydrogen amount, in which the rates increase till a maximum value at 423 K and then they decrease. The adsorption k_1 as well as irreversible binding k_2 rate constants increase independently of hydrogen percentage over the bimetallic Pt-Rh catalyst, indicating that the interaction of CO under H_2-rich conditions follows a different mechanism over the two studied catalysts.

A possible explanation for the anomalous behaviour of k_2 values, over the Rh/SiO_2 catalyst in the presence of 25% H_2, to decrease at temperatures higher than 423 K, is that the calculated rate constants for the irreversible binding of CO, k_2, are apparent ones. These are related to the true values via the equation: $k_{2(\text{true})} = k_2/K$, where K is the equilibrium constant for a possible faster reversible intermediate step (e.g. due to the formation of a surface H–CO complex which is bound weakly and desorbs more easily than adsorbed carbon monoxide, CO_{ads} [2]). Consequently, the true activation energy E_a^{true} is the sum of the apparent activation energy due to k_2 (slow process), Ea_2, and of the heat of the reversible step (faster process), ΔH. Thus, when ΔH is negative and higher in absolute value than Ea_2 the rate of the process, k_2, is expected to decease with rising temperature. The observed temperature decrease of the adsorption, k_1, and surface irreversible binding, k_2, rates of the monometallic catalyst (c.f. Fig. 3) may also explained similarly. In any case, the estimation of the activation energy is not possible when rate constants decrease.

The calculated by means of Arrhenius equation activation energies as well as their standard errors, for the adsorption (E_{a1}), desorption (E_{a-1}) and surface binding (E_{a2}) of CO over the pure Rh and Pt–Rh alloy catalysts are summarized in Tables 1 and 2, while the comparative variation of the desorption barriers (E_{a-1}) against the different hydrogen carrier-gas compositions is presented in Fig. 6.

A first characteristic of the estimated activation energies is that their values are significantly lower, compared to those mentioned in literature for SCO (74 kJ mol^{-1} over a Pt/Al_2O_3 catalyst [3]) as well as for CO oxidation (56–80 kJ mol^{-1} over Pt/γ-Al_2O_3 and Pt/SiO_2 catalysts [15–17]) and moreover also lower than those determined for CO adsorption in the absence of H_2 over the studied catalysts [6] (c.f. Tables 1 and 2). The latter is reasonable since the addition of H_2 or H_2O has been found to decrease significantly the activation energy of CO oxidation increasing the rate [3].

Table 1
Activation energies (kJ mol^{-1}) corresponding to the adsorption, E_{a1}, desorption, E_{a-1} and surface binding, E_{a2}, of carbon monoxide on the studied silica supported Rh catalyst under three different hydrogen carrier gas compositions

% H_2	E_{a1} (kJ mol^{-1})	E_{a-1} (kJ mol^{-1})	E_{a2} (kJ mol^{-1})
0	19.4 ± 6.5[a]	11.9 ± 2.2[a]	3.8 ± 1.0[a]
25	[b]	5.2 ± 0.6	3.2 ± 0.6
50	[b]	2.3 ± 0.7	[b]
75	[b]	1.4 ± 0.7	[b]

[a] Values for CO adsorption in the absence of H_2 at 553–723 K, obtained from ref. [6]. The ± values in this and the following table are standard errors.
[b] Activation energy values can not be determined.

Table 2
Activation energies (kJ mol^{-1}) corresponding to the adsorption, E_{a1}, desorption, E_{a-1} and surface binding, E_{a2}, of carbon monoxide on the studied silica supported $Pt_{0.50}$ + $Rh_{0.50}$ alloy catalyst under three different hydrogen carrier gas compositions

% H_2	E_{a1} (kJ mol^{-1})	E_{a-1} (kJ mol^{-1})	E_{a2} (kJ mol^{-1})
0	18.2 ± 2.6[a]	12.6 ± 1.7[a]	[b]
25	4.5 ± 1.1	3.0 ± 0.7	5.9 ± 1.6
50	7.6 ± 0.7	5.4 ± 0.4	5.2 ± 1.7
75	8.5 ± 1.6	4.2 ± 0.7	7.2 ± 2.8

[a] Values for CO adsorption in the absence of H_2 at 553–723 K, obtained from ref. [6].
[b] Activation energy values can not be determined.

Low activation energy values for the oxidation of carbon monoxide over noble metals have also been observed [18]. Low energy barriers especially for dissociation reactions are not strange. The geometrical effect on the dissociation barriers, i.e. lower dissociation barriers on steps, kinks and defects than that on terraces, is mainly a consequence of change in activation energy of association, particularly in interaction energy in transition state. On corrugated surfaces the reaction can achieve such transition state structures that two reactants do not share bonding with metal atoms. As a result, the association barriers will be small leading to finally lower dissociation barriers [19]. Such low activation energy values, as the estimated for the interaction of CO with the studied catalysts, may be indicative of corrugated surfaces. The catalytic activity of supported Rh particles has been related to the large number of defects that are present at the surface of such small particles [20].

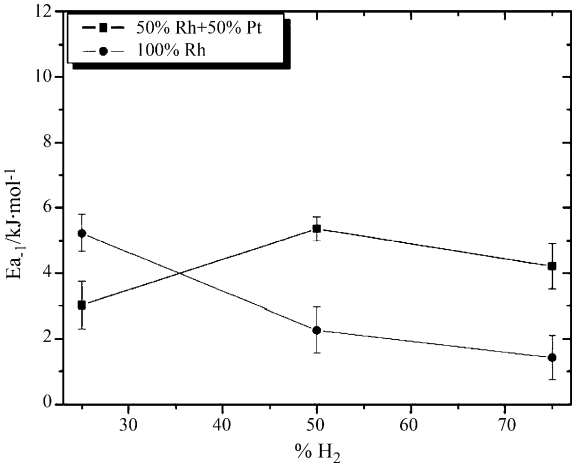

Fig. 6. Plot of the activation energy (kJ mol^{-1}) estimated by means of Arrhenius equation for the desorption E_{a-1} of carbon monoxide over the two studied silica supported monometallic Rh and bimetallic $Pt_{0.50}$-$Rh_{0.50}$ catalysts against the percentage of the carrier-gas hydrogen (25–75% H_2).

Differential heats of adsorption have strong surface coverage dependence, decreasing as the uptake increases [21]. Moreover, it is suggested that at fuel cell operating conditions in the presence of CO the coverage is higher and adsorption energies weaker. This is attributed to strong CO–CO repulsions at high coverages [4]. Most likely the calculated by means of the present methodology activation energies are referred to high surface amounts of CO. This is also ascertained from the fact that the local monolayer capacity of the Rh/SiO_2 catalyst increases from 12 $\mu mol\,g^{-1}$ to 2 $mmol\,g^{-1}$ under a change of carrier gas hydrogen amount from 25 to 75% [7].

Even though, the found activation energies were apparent ones the variation of their values versus hydrogen percentage and from one metal or alloy to the next, can give useful information for the activity and the selectivity of CO adsorption in excess of hydrogen over the studied Rh and Pt–Rh alloy catalysts.

From the values of the activation energies of Table 2, it is also concluded that the adsorption and surface binding barriers increase as hydrogen feed composition increases indicating that lower amounts of CO are more strongly bound on Pt–Rh alloy active sites, resulting in higher selectivity for SCO.

Since the activation energy for the adsorption as well as surface binding steps can not be estimated for the adsorption of CO on the monometallic Rh catalyst active sites, the comparable presentation of Fig. 5 includes only the desorption barriers (E_{a-1}). It is concluded that at the range of hydrogen compositions between 40 and 75% which is compatible with PEM fuel cells feed/streams, the activation energy required for CO desorption decreases as feed H_2 content increases indicating that desorption becomes easier and ensuring higher activity for CO oxidation. Moreover, the desorption barriers determined in the range 40–75% H_2 are in any case much lower than the respective activation energies found for CO desorption in the absence of hydrogen (c.f. Tables 1 and 2). Thus, a H_2-induced desorption of CO is reported, which could qualitatively explain the observed rate enhancement of SCO oxidation rate if we assume that CO oxidation rate is desorption limited. Hydrogen-induced desorption of CO has been reported for Pt(1 1 1) at low temperatures [22].

The physical origin of the H_2/H_2O-induced increase in SCO oxidation rate has become a subject of great interest. Various explanations have been suggested. The formation of the previously mentioned H–CO complex, due to the interaction of adsorbed CO with H_2 present in the feed gas stream, is believed to enhance the reaction by desorbing from the catalyst surface below the temperature required for CO desorption in the absence of H_2 [2]. A different explanation is attributed to the interaction between the hydroxylated supporting oxide material (Al_2O_3, SiO_2 or TiO_2) and CO adsorbed on Pt. By this process formate species are formed on the support if H_2 and/or H_2O are present in the gas feed. The formation of formate species on alumina-support consumes Pt-bonded CO producing free Pt-sites for O_2 adsorption/dissociation, effecting an increase in SCO rate [23].

5. Conclusions

An inverse gas chromatographic instrumentation, that of Reversed Flow Gas Chromatography, was used for the study of CO adsorption, which is an elementary step of selective CO oxidation (SCO), over a silica supported monometallic Rh and $Rh_{0.50} + Pt_{0.50}$ bimetallic catalysts, under various hydrogen atmospheres, varying from 25 to 75% H_2. The presented methodology is technically very simple and it is combined with a mathematical analysis that gives the possibility for the estimation of various physicochemical parameters related with the adsorption on heterogeneous surfaces in a simple experiment under conditions compatible with the operation of fuel processing catalysts. Rate constants for the elementary processes of adsorption, desorption and surface binding and the respective Arrhenius parameters are determined. For first time the effect of different hydrogen contents of the gas feed/stream in the kinetics of CO adsorption is investigated.

It is suggested in the literature that the selectivity of CO oxidation in excess of hydrogen over group VIII noble metals at temperatures lower than 523 K is determined from the strength of CO adsorption, while SCO activity by CO desorption.

The temperature variation of the rate constants reveals that the activity as well as the CO selectivity of the monometallic Rh catalyst increase with rising temperature. In contrast the activity of Pt-Rh bimetallic catalyst is expected to increase while its selectivity is expected to decrease at higher temperatures.

Monometallic Rh/SiO_2 catalyst combines high activity, increasing at rising hydrogen contents and high CO selectivity, which however decreases at increasingly H_2-rich conditions, in agreement with literature observations. In contrast, Pt–Rh alloy catalyst is expected to exhibit high CO selectivity, which increases at rising hydrogen compositions and high activity which decreases at increasingly H_2-rich conditions. The suggested CO tolerance of Pt-based alloys is not directly ascertained since comparable data for CO adsorption over Pt are not available.

At lower H_2 compositions the CO selectivity of both catalysts is expected to be similar but Pt–Rh alloy catalyst is expected to be more active in agreement with the observed Pt–Rh synergism. At higher hydrogen compositions (40–75% H_2) compatible with the operation of PEM fuel cells, the activity of both catalysts is expected to be similar but Pt–Rh alloy catalyst is expected to be more selective. Thus, Pt–Rh alloy catalyst may be considered as a better candidate for CO preferential oxidation.

The values of the experimentally determined activation energies are low compared to literature values. These low energy barrier values most likely are referred to high surface amounts of CO in agreement with it is suggested in the literature that at fuel cell operating conditions in the presence of CO the coverage is higher and adsorption energies weaker due to strong CO–CO repulsions at high coverages.

Moreover, the values of the activation energies determined under H_2-rich conditions are lower than those determined for CO adsorption in the absence of H_2 over the studied catalysts in agreement with the literature conclusions that the addition of H_2 or H_2O decreases significantly the activation energy of CO oxidation increasing the rate of SCO.

The desorption activation energy which is CO oxidation activity determining step, in the compatible with the operation of PEM fuel cells composition range 40–75% H_2, decreases as feed % H_2 content increases. Moreover, the desorption barriers determined are in any case much lower than the respective activation energies found for CO desorption in the absence of hydrogen indicating a H_2-induced desorption, which can explain the observed rate enhancement of SCO oxidation.

References

[1] A.F. Ghenciu, Curr. Opin. Solid State Mater. Sci. 6 (2002) 389.
[2] S.H. Oh, S. Sinkevitch, J. Catal. 142 (1993) 254.
[3] M.J. Kahlich, H.A. Gasteiger, R.J. Behm, J. Catal. 171 (1997) 93.
[4] P. Liu, A. Logadotir, J.K. Norskov, Electrochim. Acta 48 (2003) 3731.
[5] D. Gavril, J. Liq. Chromatogr. Related Technol. 25 (2002) 2079.
[6] D. Gavril, V. Loukopoulos, G. Karaiskakis, Chromatographia 59 (2004) 721.
[7] V. Loukopoulos, D. Gavril, G. Karaiskakis, Instrum. Sci. Technol. 31 (2003) 165.
[8] D. Gavril, Instrum. Sci. Technol. 30 (2002) 397.
[9] D. Gavril, B.E. Nieuwenhuys, J. Chromatogr. A 1045 (2004) 161.
[10] V. Loukopoulos, D. Gavril, G. Karaiskakis, N.A. Katsanos, J. Chromatogr. A 1061 (2004) 55.
[11] F.C.M.J.M. Van Delft, B.E. Nieuwenhuys, J. Siera, R.M. Wolf, I.S.I.J. Int. 29 (1989) 550.
[12] G. Karaiskakis, D. Gavril, J. Chromatogr. A 1037 (2004) 147 (Review).
[13] N.A. Katsanos, R. Thede, F. Roubani-Kalantzopoulou, J. Chromatogr. A 795 (1998) 133.
[14] Y.E. Li, D. Wilcox, R.D. Gonzalez, AIChE J. 35 (1989) 423.
[15] N.W. Cant, P.C. Hicks, B.S. Lennon, J. Catal. 54 (1978) 732.
[16] N.W. Cant, J. Catal. 62 (1980) 173.
[17] J. Sarkany, R.D. Gonzales, Appl. Catal. 5 (1983) 85.
[18] A. Baiker, M. Maciejewski, S. Tagliaferri, P. Hug, J. Catal. 152 (1995) 407.
[19] Z.P. Liu, P. Hu, J. Chem. Phys. 114 (2001) 8244.
[20] M. Mavrikakis, M. Baumer, H.J. Freund, J.K. Norkov, Catal. Lett. 81 (2002) 153.
[21] H. Rong, H. Kusaka, M. Mavrikakis, J.A. Dumesic, J. Catal. 217 (2003) 209.
[22] D.H. Parker, D.A. Fisher, J. Colbert, B.E. Koel, J.L. Gland, Surf. Sci. 258 (1991) 75.
[23] H.S. Murray, Fuel Cell Seminar, Book of Abstracts, in: “Fuel Cell”, sponsored by the National Fuel Cell Coordinating Group, Tucson, AZ, 1985, p. 129.